ELSEVIER

Journal of Nuclear Materials 265 (1999) 124–133

journal of nuclear materials

Effect of fast Ti-deposition on gas recycling at the first wall and on fast ion losses in the GDT experiment

P.A. Bagryansky [a,*], E.D. Bender [a], A.A. Ivanov [a], A.N. Karpushov [a], S.V. Murachtin [a], K. Noack [b], St. Krahl [b], S. Collatz [b]

[a] *Budker Institute of Nuclear Physics, Prospect, Lavrent'eva 11, 630090, Novosibirsk, Russian Federation*
[b] *Research Center Rossendorf, Inc., P.O. Box 510119, D-01314, Dresden, Germany*

Received 1 July 1997; accepted 2 September 1998

Abstract

Fast Ti-deposition was applied in the gas-dynamic trap (GDT) facility in the regimes with 14–17.5 keV, 2.5–4 MW neutral beam (NB) injection to control gas recycling at the first wall and thereby reduce charge-exchange losses of energetic ions. The charge-exchange losses of the fast ions turned out to be much less than in former, non-conditioned discharges. The temporal and spatial variation of the neutral gas density was measured during typical shots and compared with the results obtained by means of a Monte Carlo transport code. The comparison of the numerical results with the experimental data shows that the recycling coefficient of the chamber wall which has been freshly coated by titanium is close to that of the pure metallic surface.

1. Introduction

Coating of the first wall by titanium, carbon or beryllium films is widely used in fusion devices to reduce release of the impurities from the wall and, thereby, to improve the plasma confinement. The wall conditions are particularly important in experiments with neutral beam (NB) injection, as for instance at the Gas Dynamic Trap (GDT) [1–3], when the first wall is exposed to a high flux of secondary, high-energetic neutrals from the plasma.

At the GDT, the application of traditional methods of wall conditioning faces certain difficulties because of specific technical features of the vacuum chamber design. In particular, all connections use elastomer sealings. Thus, the chamber cannot be baked at sufficiently high temperature for degassing. Therefore, ultimate pressure in the chamber with turbo-molecular pumping turns out to be relatively high, of the order of 10^{-4} Pa, so that during the time period between experimental shots many monolayers of residual gases cover the first wall. Since these monolayers have quite small surface binding energy, this provides a high recycling, i.e. a neutral, striking the wall, can release a lot of gas molecules. As a result of this, plasma confinement may deteriorate due to increased charge-exchange and radiative losses. In fact, this was observed in the experiments at GDT device in which the plasma is sustained during a few milliseconds. Formerly, the experiments were carried out without a special conditioning of the chamber walls. It was observed that during the NB injection, the vacuum conditions significantly deteriorated because of a huge amount of gas released from the wall by the bombardment with high-energetic neutrals from the plasma. This observation demonstrated that a clean wall surface is an essential constraint for attaining sufficiently low charge-exchange losses for the fast ions.

The present paper is devoted to the studies of the neutral gas behavior and charge-exchange losses to fast ions under the condition, when a titanium film has been deposited on the container wall of the central cell. In order to prevent the accumulation of some gas monolayers prior to plasma shot, the deposition of titanium films on the first wall was made sufficiently fast using an

* Corresponding author. Fax: +7-3832 342 163; e-mail: p.a.bagryansky@inp.nsk.su.

0022-3115/99/$ – see front matter
PII: S0022-3115(98)00510-8

array of pulsed electric-arc evaporators [4,5]. The time between arc-evaporator's pulse and experimental plasma shot can be minimized to few hundreds of millisecond. In the case of thermal evaporators this time is determined by cooling time which is much longer.The objectives of the work are as follows:

1. to optimize the first wall pre-conditioning and the titanium deposition using arc-evaporators;
2. to reduce the charge-exchange losses of the fast ions by a higher vacuum and by a smaller gas release from the wall during the shots;
3. to compare measured dynamic gas densities with the results of calculations and, thus, to determine the recycling characteristic of the Ti-coated chamber wall.

The paper is organized as follows. In Section 2 a brief description of the GDT facility is given with an emphasis on the characteristics of vacuum and Ti-gettering systems. Sections 3 and 4 contain descriptions of the wall pre-conditioning and vacuum conditioning procedures. Section 5 describes plasma diagnostics and system which monitors vacuum conditions during plasma shot. Experimental results are presented in Section 6. The Section 7 discusses the experimental results in comparison with the predictions of Monte Carlo simulations of the neutral transport in the GDT.

2. Experimental layout

The GDT is an axisymmetric, long magnetic mirror device which is operated with a hydrogen plasma. Descriptions of plasma confinement and stability in the device are given elsewhere [1]. Its layout is shown in Fig. 1. Table 1 lists the main parameters of the facility.

The main objective of the GDT experiments is to study the basic physical phenomena underlying the project of a 14 MeV neutron source [6] dedicated for fusion materials irradiation testing. Essentially, this assumes that energy balance and stability of high plasma beta neutral-beam-heated plasma are to be studied.

2.1. Scenario of the experiment

A collisional plasma with the fast ion minority is confined in a long solenoidal central cell (1) with mirror plugs at both ends (17) [2, 3]. The plasma start-up is accomplished during 3.5 mc by injecting a plasma along the field lines from one end. For that purpose a gas-puffed washer-stack plasma gun (4) is installed inside the end tank (see Fig. 1). High current arc discharge in the gun is fed by hydrogen in the amount of 1–5 Torr l per plasma shot. According to special measurements the gun-produced plasma is highly ionized (>99.9%). In fact, the gas puffing into the gun does not provide substantial increase in the central cell pressure during a shot, because of a sufficiently low gas conductance between cells through the linking mirror throat (<500 l/s for hydrogen). Subsequently, the target plasma column with an initial temperature of 3–5 eV and density of 6×10^{13}–10×10^{13} cm^{-3} is heated up by NB injection which at the same time provides the desired fast ions. The typical time of NB-injection is 1.2 ms. The lifetime

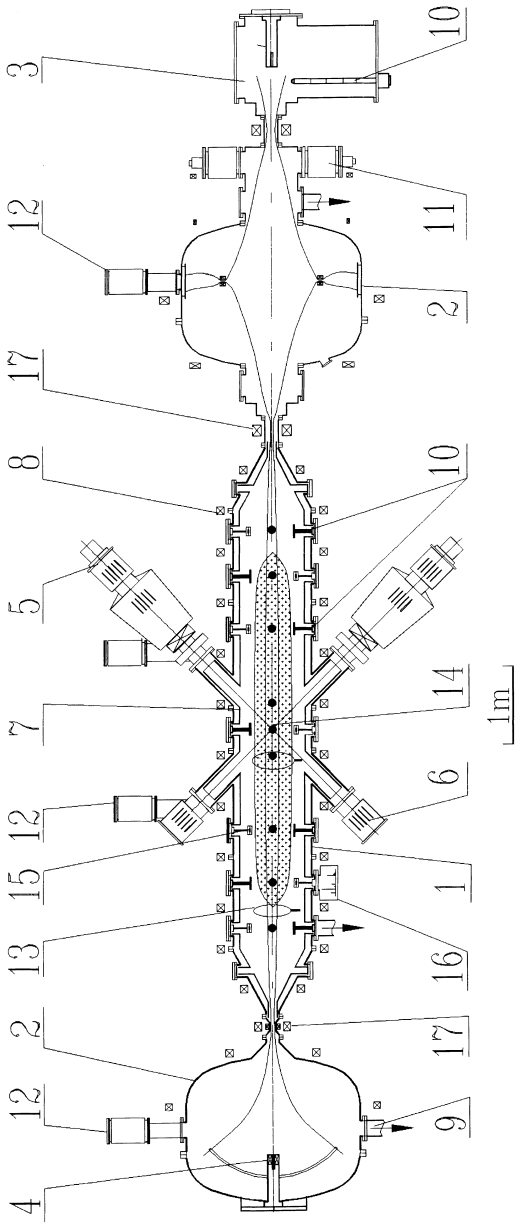

Fig. 1. The GDT layout: 1 – central cell; 2 – end cells; 3 – plasma dump; 4 – plasma gun; 5 – NB-injectors; 6 – NB-dumps; 7 – internal liner plates; 8 – magnetic field coils; 9 – turbomolecular pumps; 10 – Ti-evaporators; 11 – Ti-getter pumps; 12 – liquid helium pumps; 13 – diamagnetic loops; 14 – bolometers; 15 – FIMIG; 16 – QMA, 17 – mirror plugs.

Table 1
The GDT parameters

Parameter	Value
Mirror-to-mirror	7 m
Magnetic field at midplane	up to 0.22 T
In mirrors	2.5–15 T
Density of the target plasma	0.1×10^{14}–1.5×10^{14} cm^{-3}
Radius of the target plasma	8–15 cm
Injection energy of NB	14–17.5 keV
Pulse duration of NB	1.2 ms
Total injection power of NB	2.5–4 MW
Injection angle of NB	45°
Peak density of fast ions	Up to 10^{13} cm^{-3}
with mean energy	4.5–5.5 keV

of fast ions depends on drag rate on electrons, Coulomb scattering rate and charge-exchange rate. Typically the lifetime is 500–600 μs. The NB deposition is not completely axisymmetric. Six NB-injectors (5) are azimuthally arranged in two groups on opposite sides of the central cell. The azimuthal angle between injectors in the group is 30°.

2.2. GDT vacuum system

The GDT vacuum vessel consists of three main chambers: a central cell confining the main plasma and end cells attached to both ends of the central cell. The central cell volume, including the injector ducts is 9 m^3. The volume of the end tank containing the plasma gun amounts to 5 m^3. The opposite tank which is 5.5 m^3 in volume, houses a cusp cell. Diameter of the opening inside the mirror plugs is about 80 mm, gas conductance between the three chambers estimates as 500 l/s for H_2. It is important to note, that the inner walls of vacuum vessel close to mirror plugs act as plasma limiters. The material of the limiter is stainless steel coated by titanium. All the joints that require periodical connections and disconnections are made with the elastomer sealings. The central cell and the end chambers are pumped out by 1.5 m^3/s turbomolecular pumps each. Additionally, there are installed four 2.5 m^3/s liquid helium cryopumps. Two of them are located in the central cell, the others in the end cells. Additionally, there are also liquid nitrogen (LN) cooled water traps inside the central cell with a pumping speed of about 3.5 m^3/s (for water vapor). The end cells are additionally equipped with pulsed Ti-getter pumps containing LN-panels inside [5]. They add 2.5 m^3/s each. Three of them are installed in the end tank housing the plasma gun.

The volume of the injector beamlines is 0.3 m^3 each. In order to prevent the hydrogen which is puffed inside the injectors, to enter the central cell during a plasma shot, baffles are installed in the duct between the neutralizer and the chamber entrance. These baffles are oriented along the beam particle trajectories so that the projected beam transparency of 0.98 is preserved. On the other hand, the gas conductance is significantly reduced as desired. In that way a time delay of the gas puff diffusion into the central cell exceeding 10 ms has been achieved. This measure the gas source from the beamlines became less than other sources. The beam dumps which are located facing the injectors are also equipped with baffles of similar design to provide the required delay of the gas released from its surfaces.

In experimental runs the NBS are injected in intervals of 60 s to control the grid's conditions. Each shot of NB-injectors introduces about 3×10^{19} hydrogen molecules into the chamber. The interval between plasma shots is longer, and amounts to 5 min. Taking into the account the additional gas from the plasma gun, one can estimate that the total amount of gas entering the GDT vacuum vessel during a plasma shot is about 2×10^{20} molecules.

2.3. First wall liner

In order to improve wall conditions in the central cell of the vacuum chamber Ti-evaporators have been installed which are capable of depositing a sufficiently thin metallic film on the inner surface of the chamber in short time. Problems can occur with a metallic film deposited by an electric-arc evaporator with high evaporation rate. Blistering and shrinking of the film often occur, especially, if the film thickness exceeds 0.1 mm. Moreover, unless special precautions have been taken the film may detach from the wall. To minimize this risk a specially prepared stainless steel liner has been mounted on the inner wall surface of the central cell. The liner consists of 2 mm thick panels directly bolted to the chamber walls. Before mounting (just once), the plates have been gone through sand blasting, washing with distilled water and continuous baking in vacuum at 450°C. By the sand blasting the surface of the plates became rough and so effectively enlarged about 1.4–2 times. The advantage of the higher surface roughness of the plates is twofold, both the adhesion of the coated Ti-film to the plate and its pumping rate are increased [5]. It is important to note, that baking procedure is not used. The temperature of vacuum vessel and liner plates is close to the room temperature.

2.4. Ti-evaporators

In order to deposit the film homogeneously into the liner surface totaling 21 m^2 arc Ti-evaporators are installed in the central cell at nine locations along the axis (see (10) in Fig. 1.). The layout of an arc-evaporator is schematically shown in Fig. 2. [4]. The exhaustible titanium body of the evaporator consists of three radial sticks which are connected in the joint middle (2). The ends of the sticks are connected to the phases of a three

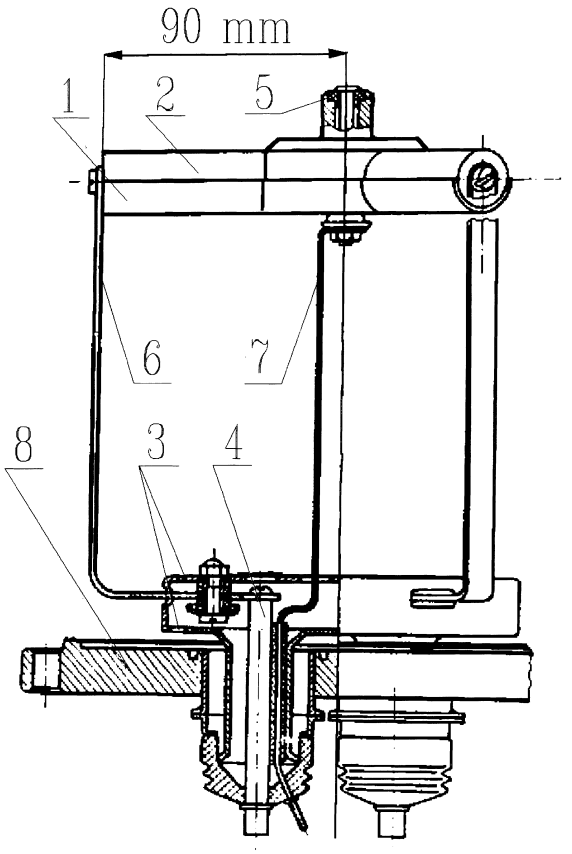

Fig. 2. The layout of an evaporator: 1 – Mo-shield; 2 – Ti-electrode; 3 – stainless steel shield; 4 – Cu-conductor; 5 – trigger device; 6 – Mo-conductor; 7 – trigger conductor; 8 – flange.

phase voltage supply line. The cathode spots are fixed on the surface of the rods by virtue of their reverse motions in the magnetic fields which are produced by the oscillating currents flowing along the rods. Such a design of the evaporator ensures a homogeneous consumption of the rods. On their back sides the rods are protected by a molybdenum shield (1) which prevents the spots from entering back to the upper side. The arc is initiated by a trigger (5) in which a breakdown occurs over the surface of a ceramic ring insulator. Trigger voltage pulse is supplied through a special feed (7). The duration of the arc discharges is varied by switching off and on the thyristors in the phases of the supply line. The evaporators are operated in a pulse mode, therefore, their averaged current appears to be small enough. The moderate mean power consumption of the evaporators makes it possible to use just three 2.5 kVA three-phase transformers to supply them all.

The current through one evaporator typically amounts to 300–400 A that corresponds to 15–20 μg/s evaporation rate. To deposit a Ti-film on the liner the evaporators are switched on for 0.25 s. This procedure produces a film of a mean thickness of about 3 Å. Special flaps which are driven by an joint pneumatic-system are used to prevent the Ti-coating of the probes, optical ports, and other sensitive parts of the diagnostics located in the central cell. There are also several movable diagnostic elements that are installed on feedthroughs driven by computer controlled step motors. Before starting the deposition procedure these diagnostics are retracted into regions protected by special shields.

3. Liner pre-conditioning procedure

After installing the liner plates, a special pre-conditioning procedure has been accomplished to improve adhesion of Ti-film. First, the chamber was pumped out and the first wall pre-conditioning was performed by a sequence of glow discharges. The glow discharge cleaning was applied just once after the liner installation. Discharges were initiated by an array of five passively cooled anodes mounted in the central cell. The first stage of glow discharge cleaning was carried out with argon at 200 Pa pressure and continued 12 h. Subsequently, the cleaning was continued in hydrogen at the same pressure also for about 12 h. This cleaning procedure was finished when the time integrated current density of the discharge exceeded 0.4 C/cm^2 (in equal amounts for the discharges in both gases).

At the GDT facility the Ti-gettering system has been operated during the last three years. About 3×10^4 cycles of evaporation were done so far. The mean thickness of the totally deposited film is estimated to be about 10 μm. Until now there are no observations that the titanium film detaches from the wall. This is confirmed by the regularly monitored radiation losses of the plasma which are negligibly small proofing that there is no considerable amount of titanium dust inside the system.

4. Vacuum conditioning

The typical procedure for preparing the required vacuum conditions to experiments after every opening the device to air includes:

1. the chamber is evacuated by a mechanical pump that typically takes 1.5–2.5 h;
2. the preliminary pumping by turbomolecular pumps during 2–3 h, the base pressure at the end of this phase attains 1×10^{-3}–3×10^{-3} Pa;
3. the high vacuum pumping using turbomolecular pumps and LN-traps usually takes 3–5 h what lowers the pressure to 2.7×10^{-4}–5.6×10^{-4} Pa;
4. the Ti-evaporator system deposits the titanium simultaneously on the central cell wall, on the surface of the Ti-getter pumps and on the walls of the plasma dump chamber located beyond the cusp end tank

(see Fig. 1 for details). At the beginning, the evaporators are periodically turned on in intervals of 30 s. After half an hour the intervals are enlarged up to 60 s and after another half an hour – up to 100 s. In this way, after 2–5 h the base pressure decreases to 2.7×10^{-5}–6.5×10^{-5} Pa. Upon completion of this stage a few tens plasma shots are made for additional wall conditioning. At the beginning the shots are made with the gun-produced plasma solely, later on the NB injectors are turned on, too. After continuous pumping by means of all pumping tools mentioned before the base pressure in the central cell attains 1×10^{-5}–2.7×10^{-5} Pa.

5. At this stage, additionally, the cryopumps may be filled with liquid helium. when the helium is overcooled by pumping out helium vapor from the cryopumps the central cell pressure reaches 4.9×10^{-6}–6.5×10^{-6} Pa.

During routine operation without exposing the chamber to air, the procedures 2–4 or 2–5 are repeated as follows: initial pumping (2) – 1 h; high-vacuum pumping (3) – 0.5 h; Ti-gettering (4) – 1 h.

After 5–10 experimental shots the evaporation system starts and deposits the titanium by 10–30 pulses. The base pressure during the experiments is sustained at a level of about 0.5×10^{-5}–1.1×10^{-5} Pa depending upon whether the helium cryopumps operate or not.

5. Vacuum monitoring and plasma diagnostics

The base pressures in eight regions of the GDT vacuum chamber are monitored by standard inverse magnetron ionization gauges with a time resolution of 2 s. To measure dynamic gas pressure during a plasma shot five fast inverse magnetron ionization gauges (FIMIG) are used. They are installed 20 cm distant from the wall in the axial locations shown in Fig. 1. The measured individual sensitivity of the FIMIGs was different depending on the magnetic field inside the gauge and on its precise dimensions which slightly vary. Their values are in the range of 5–20 mA/Pa. The time resolution of the FIMIGs was measured to be about 150 μs.

The charge-exchange and radiation losses from the plasma were measured by means of a set of pyro-bolometers. The time resolution of the bolometers is 10 μs. Fig. 1 shows the location of the bolometers in the central cell. Near to the midplane the fast ions are neutralized by charge-exchanging with neutral particles and leave the plasma within a rather small interval of pitch angles near the injection angle of 45°. Because of this, here we are able to separately measure charge-exchange losses of fast ions and radiative losses from the plasma. For this purpose, the bolometer located at the midplane is used in conjunction with a movable collimating tube aimed on axis (Fig. 3). If the collimator is moved outwards to the extreme radial position, an acceptance angle of the bolometer is large enough (close to 2π), so that the bolometer sees the radiative losses from the entire plasma column as well as the charge-exchange fast neutrals. In the down position, the collimator prevents the fast neutrals (with pitch angles near 45°) from entering the bolometer. Hence the charge-exchange losses are not observed. At the same time, the solid angles at which the bolometer views the plasma in both positions of the collimator do not differ significantly, so that the measured radiative losses are kept almost constant. This permits a differentiation of the central cell plasma radiative losses from the charge-exchange losses.

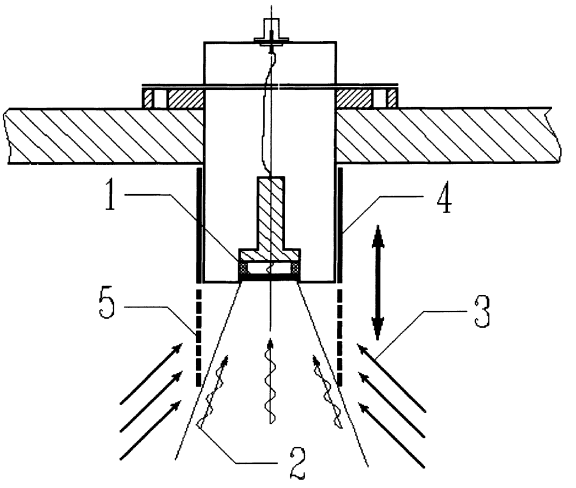

Fig. 3. The layout of the pyro bolometer installed near the midplane: 1 – pyro bolometer; 2 – radiation flux from plasma; 3 – charge-exchange neutrals (pitch-angles close to 45°); 4,5 – the extreme positions of the collimator.

Thus, near the midplane radiative and the sum of charge-exchange and radiative losses can be measured in subsequent shots. To measure the radiative losses from the entire plasma in the central cell, we additionally use bolometers located beyond the turning point of the energetic ions in the region where charge-exchange losses become negligibly small compared to radiative ones. It was observed that in the regimes under consideration the charge-exchange losses are dominant. The energy contents of the target plasma and of the fast ions were determined by the diamagnetic loops located at the midplane and beyond the turning point of the fast ions.

Using the measured energy contents W_f and the charge-exchange losses P_{ex} of the fast ions their effective charge-exchange energy lifetime τ_{ex} was calculated as the ratio of the two quantities $\tau_{ex} = W_f/P_{ex}$ and then used to characterize the vacuum conditions before and after the installation of the Ti-evaporation system.

The profiles of plasma density and temperature were measured using movable triple probes, the Thomson

scattering system and the array of NB attenuation detectors. NB attenuation detectors are also used to measure the trapped power of NB. These data were used (see Section. 7) in the calculations of the hydrogen gas and fast ions using the Fast Ion Transport code, FIT [7].

6. Experimental results

The hydrogen pumping rate of the deposited titanium film was measured by pulsed puffing of hydrogen into the central cell and subsequent measurements of the characteristic pressure drop time. By these measurements the pumping rate of the titanium film has been estimated to be 1.5–2 1/s cm^2 that is in a reasonable agreement with the data for a pure titanium surface at room temperature [8]. It is worthwhile to note that this figure has not changed since the last three years of operation with the Ti-coated container wall at the GDT facility.

Residual gases are monitored by a quadrupole mass-analyzer (QMA) installed in the central cell of the GDT. Oxygen, nitrogen, water, and methane are the dominant gas components. The QMA registers their almost equal partial pressures in shot-to-shot intervals. After a plasma shot, the partial pressures of hydrogen builds up by two orders of magnitude higher than that of the other gases and thus we took the hypothesis that also during a shot all other gases but hydrogen may be neglected in calculations of charge-exchange losses of fast ions. As yet this was not directly verified by the measurements of partial pressures of other gases but hydrogen during a shot. Nevertheless, this hypothesis is supported by reasonable agreement between measurements of dynamic pressures in the different points inside the central cell and calculations of hydrogen behavior during a shot (see Section 7 for details).

Total NB power in excess of 4 MW (for 14–17.5 keV beam energies) is injected into the central cell during 1.2 ms. About a half of the injected power is trapped due to charge-exchange and ionization collisions with target plasma particles providing fast ions build-up. The fast ion density was measured by making use of an array of diamagnetic loops installed at different axial locations coupled with the measurements of the energy and angular distribution of fast ions at the midplane. According to these measurements, by the end of the injection the fast ion density reaches 10^{13} cm^{-3} in vicinity of the turning points. The temporal behavior of the injected and trapped NB power is shown in Fig. 4. In recent experiments [3], after Ti-evaporators have been employed, a temperature of the collisional target plasma exceeding 100 eV was measured. The energy spectra of the fast ions covers the whole range up to the injection energy. The mean energy of fast ions was measured to be 4.5–5.5 keV.

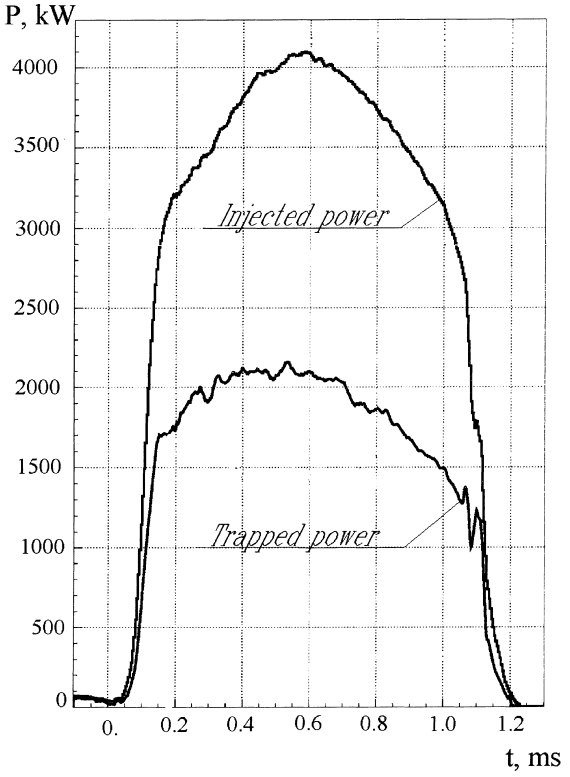

Fig. 4. Time evolution of the injected and trapped NB power.

Temporal variation of the charge-exchange and radiative losses in a typical shot is shown in Fig. 5. It is worthwhile to note that these were much smaller than trapped NB power.

The charge-exchange lifetime of the fast ions (defined as in the previous section) measured in reference shots before the installation of the Ti-gettering system and after that is shown in Fig. 6. One can see that with a

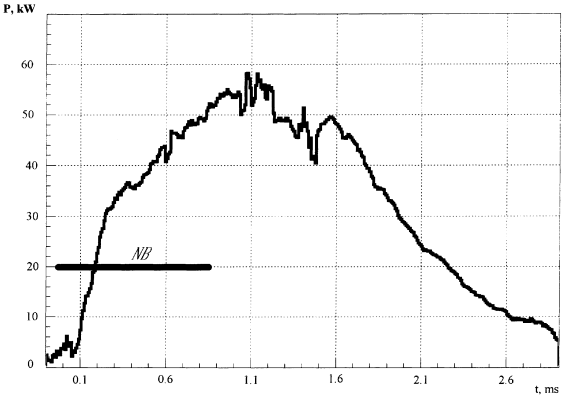

Fig. 5. Temporal variation of total charge-exchange and radiative losses during plasma shot.

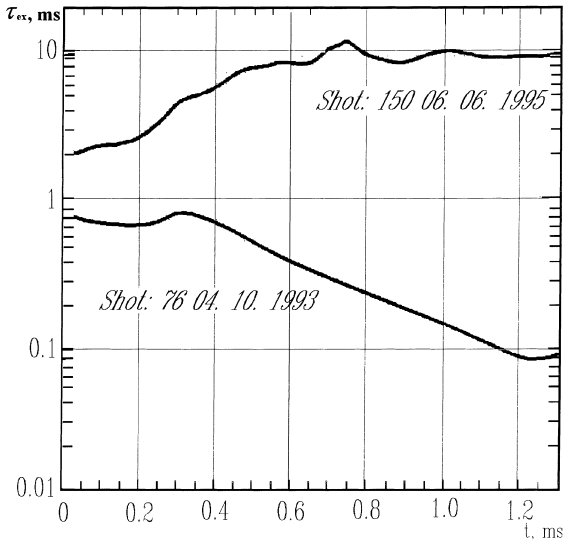

Fig. 6. Charge-exchange lifetime of the fast ions before (SHOT:76) and after (SHOT:150) Ti-gettering.

titanium film on the wall the charge-exchange lifetime of fast ions increases to nearly 10 ms. In contrast to that, in the reference shots without Ti-gettering the charge-exchange lifetime was decreasing during the injection pulse due to strong gas release from the wall caused by the bombardment with energetic neutrals. That is, the gas recycling at the wall has been significantly reduced by the titanium evaporation and, consequently, the charge-exchange losses of the fast ions have been decreased by about two orders of magnitude and became negligible in their energy balance, whereas in non-conditioned shots those were dominant [2].

The temporal variation of the gas density was measured by the FIMIGs. Fig. 7 shows the results measured at the midplane for two regimes. The one, marked as 'fresh' Ti-film, was recorded 5 min after the Ti-evaporation and the other, marked as 'old' Ti-film, 1 h after that. It is clearly seen from Fig. 7 that continuous exposing of the film to residual gases atmosphere results in significant (4–5 times) increase of number of neutral particles released during plasma shot.

7. Discussion

The presented data clearly indicate that fast Ti-deposition on the liner significantly improve wall conditions at GDT. The wall conditions may be characterized by the recycling coefficient γ defined similarly as in [9]

$$\gamma = \frac{\text{reflected neutral atoms} + 2 \times \text{molecules leaving wall}}{\text{neutrals striking wall}}$$

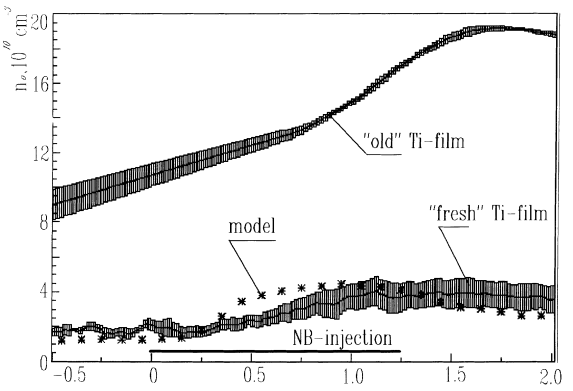

Fig. 7. Density variation at the GDT midplane measured by FIMIG and that simulated by TUBE.

For a pure metallic wall the recycling coefficient is constrained to be within the limit $\gamma \leqslant 1$ in contrast to the case of wall covered by monolayers of gas molecules when $\gamma \geqslant 1$ can be realized. To compare the properties of the fast deposited Ti-film with those of pure metallic surface the neutral gas evolution during a shot was calculated by means of the neutral transport code TUBE and the FIT code [7]. TUBE performs the Monte Carlo simulation of the time-dependent, linear neutral particle transport inside a metallic container which may be composed by an arbitrary sequence of cylinders and cones. At present, only the coupled transport of hydrogen atoms and molecules may be simulated. Their interactions with the hydrogen plasma and the container walls are dealt with analogously as by the EIRENE code [10,11] that has been developed for solving neutral gas problems in tokamaks. The data necessary for the simulation of the relevant processes are taken from [12–19]. TUBE supposes an independent, axisymmetric and maxwellized target plasma to be given by density and temperature distributions. At present, during their random walk the hydrogen atoms and molecules interact with this target plasma only but not with the fast ions that are injected into the system by the high-energetic NB injectors. The interaction processes taking into account by TUBE include absorption, i.e., ionization by electron and ion impact and scattering by charge-exchange with the plasma ions.

The neutral gas inside the GDT facility consists of several components which are produced by different sources. Particularly, in the simulations performed the following sources were included:

1. The residual gas source. It starts hydrogen molecules with isotropic flight directions from space points equally distributed inside the central cell of the GDT. Their energy distribution corresponds to room temperature.

2. The plasma-limiter source. This starts neutrals from the surface of radial limiters as result of the

following procedure. According to the information on the target plasma an ion is randomly selected in the near neighborhood of the limiter, then accelerated perpendicularly to the surface by a sheath potential of $(4.6 \pm 0.1) \times T_e$ (as measured at the GDT) and after that processed by the necessary wall reflection model for atoms.

3. The charge-exchange source. This source is given as a multitude of birth points with the necessary cinematic parameters for the neutrals to be started. This option is used for both the 'warm' neutrals generated by charge-exchange processes of the injected NB at the target plasma ions and for the 'fast' neutrals that were born during the transport of the fast ions by charge-exchanging with the neutral gas. The required data are generated by the FIT code using measured parameters of the target plasma and injected beams as inputs.

To separate contribution of each neutral gas component the calculations were carried out for each source separately. The residual gas calculation starts just at the beginning of the plasma gun operation 2 ms before the NB injection. The initial conditions are determined by the measured value of the gas pressure inside the central cell. The limiter gas calculation also starts with the plasma gun. The necessary information for the source are completely extracted from the measured density and temperature distributions of the target plasma. The NB injection generates the sources of the warm and fast neutrals. The first one terminates with the NB injection whereas the other falls off with the number of fast ions inside the system. The source distribution of the fast neutrals was produced by a FIT calculation. In this simulation the neutral gas had been approximately modeled by TUBE results for the warm gas components. All calculations were extended up to 2 ms after the start of the NBs.

The TUBE code differently simulates the interactions of atoms and molecules with the Ti-coated container wall. Molecules are of low-energy which is determined by the wall temperature. Therefore, a molecule striking the surface is assumed not to penetrate into the wall but to detach just one molecule which has been adsorbed on the surface. The flight direction of the secondary molecule is randomly selected from a cosine-distribution relatively to the surface normal and the energy is that of the incident molecule. Contrary to that the reflection model used for atoms is a more complicated one. Furthermore, there is a certain arbitrariness caused by the remarkable lack of data for incident energies below 10 eV. Using published data the following simulation scheme has been incorporated in TUBE. Assuming a hydrogen atom striking the surface with energy E^{inc} and statistical weight WT^{inc} then one H-atom is reflected with the weight $WT^{refl} = WT^{inc} \times R_N(1 - P_{abs})$ and with the energy $E^{refl} = E^{inc} \times R_E$. Furthermore, a molecule is emitted with the weight $WT^{refl}_{H_2} = WT^{inc} \times (1 - R_N) \times (1 - P_{abs}) \times 1/2$. Here $R_N(E^{inc})$ and $R_E(E^{inc})$ are the particle and energy reflection coefficients, respectively [15,16], pabs – absorption probability. With $P_{abs} = 0$, the model corresponds to a 'saturated wall'. For atoms with $E^{inc} < 10$ eV TUBE offers also the model of a 'pumping wall' that absorbs atoms with the probability $P_{abs} = \exp(-E^{inc}/E^s)$ where E^s is the surface binding energy. In calculations the value = 1 eV was used for titanium.

The distribution of the secondary flight direction is a superposition of the specular and the cosine distributions [10,11]. The calculations were perfomed with the mixing parameter of 0.5.

For the given plasma and injection conditions the time evolutions of the various neutral gas components inside the central cell were simulated by means of TUBE. Especially, the dynamic gas densities at the various detector positions were calculated. In these calculations the chamber wall was approximately modeled as a closed cylindrical and conical surface without the manifold entrances of the diagnostic and NB injection systems. For the midplane detector the results of that calculation with the wall reflection model 'with absorption' are also presented in Fig. 7. The results obtained with the saturated wall model are only slightly higher. The good agreement between numerical and experimental results allows to draw two conclusions, firstly, that a fresh Ti-film may be characterized as a clean titanium wall with a recycling coefficient $\gamma \approx 1$ and, secondly, that other gas sources have a negligible effect on the fast ions.

From the measured data with the old Ti-film one can roughly estimate that after 1 h $\gamma \approx 3$–4 has been reached. Under the conditions before the installation of the Ti-evaporation system the value of the effective recycling coefficient is estimated to be $\gg 1$.

For the central region Fig. 8 shows the time behavior of the gas components that are generated by the different sources modeled by TUBE. Especially, two facts are to be emphasized, namely, that during the fast ion peak the

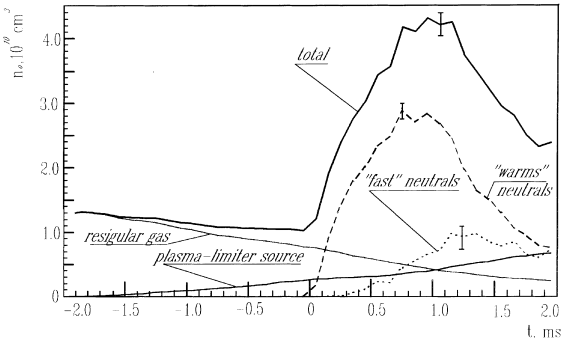

Fig. 8. Temporal variation of the neutral gas components density simulated by TUBE code at midplane of the GDT.

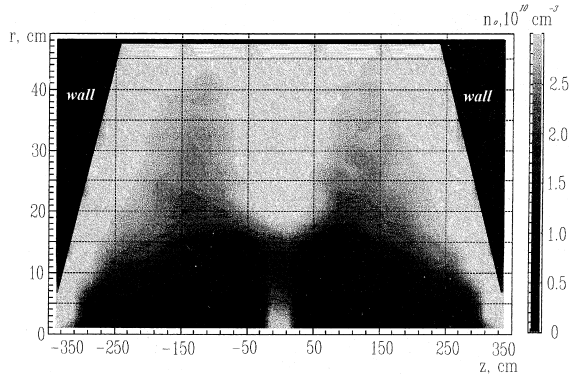

Fig. 9. Simulated spatial profile of neutrals in GDT at the final stage of NB injection.

component of the warm neutral source gives about 70% of the total gas density and that the contribution from the plasma-limiter source amounts merely 10%. The latter results from the circumstance that this source is built by the plasma streaming on the inner wall near to the mirror plugs and, therefore is located far from the center and, additionally, the relatively narrow chamber with the plasma column inside reduces considerably the gas conductance. Fig. 9 presents the calculated r, z-profile of the total neutral gas at the time 0.8 ms after start of NB injection ($z-$ is directed along magnetic axes of the GDT facility, $z=0$ corresponds to the midplane, $z=\pm 350$ cm are z-coordinates of mirror plugs and limiters). The picture illustrates that to great extent the central part of the plasma column is well-shielded by the plasma itself but with two exceptions. These are the regions near to the mirror which are fed by the limiter sources and the region near to the midplane which is fed by the warm neutral source. According to the experimental data confirmed by simulations only the latter is of importance for the fast ions.

8. Conclusions

The study of the fast ions is one of the main objectives of the GDT experimental research program. In order to decrease the charge-exchange losses of the ions, the reduction of the neutral recycling at the chamber wall is an essential demand. For that purpose, an array of Ti-evaporators of electric-arc type has been installed inside the central cell of the device. This system and its application procedure have been optimized to allow the fast (just before experimental shot) and homogeneous coating of the wall surface at any time. To improve the adhesion of the film on the background wall, the inner surface of the chamber has been covered by stainless steel panels which were undergone several special treatments. After three years of operation it has been established that the evaporation system works with high reliability and that no titanium has come off until now.

The evolution of the neutral particles in the presence of NB injection has been studied by special measurements and by means of Monte Carlo codes. The reasonable agreement between experimental and numerical results in the case of fresh Ti-films allows to conclude that for those the recycling coefficient of the fast neutrals, the energy of which covers the range of (0.1–15) keV, is close to unity what had not been the case before the installation of the Ti-evaporation system. This fact also implies that the evaporated titanium film has, within measurement and calculation accuracy, the same neutral recycling properties as pure metallic titanium. The installed evaporation system allows to perform experiments with NB injection producing fast ions with a mean charge-exchange lifetime of $\approx$10 ms that has been mainly achieved by the drastic reduction of the fast neutral recycling at the chamber wall. The reasonable agreement in time evolution of neutral gas field, which was obtained both as result of experiment and computer simulations, is also the reasonable argument to confirm the hypothesis, that gases other than hydrogen can be neglected during the discharge.

Note that the described method of electric-arc coating can be used for pulse coating of the first wall by graphite, molybedenum, niobium and other metals as well as for the fast forming of the multilayer coverings.

Acknowledgements

The authors gratefully acknowledge Dr A.M. Kudryavtsev and Dr D. Reiter for their valuable contributions to the development of TUBE code, the scientists from the GDT experimental group for their encouragement and helpful discussions. One of the authors (A.K.) is grateful to the German Academic Exchange Service for the financial support of his scholarship in the FZ Rossendorf. The work was performed in part under the auspices of INTAS (research grant No. 0013-94) and of the Saxonian Ministry of Science and Art (research project No. 7541.83).

References

[1] V.V. Mirnov, D.D. Ryutov, Sov. J. Vopr. Atomn. Nauki Tehn. -Termoyad. Sintez 1 (1980) 57.
[2] A.V. Anikeev, P.A. Bagryansky, E.D. Bender et al., Proc. of 23th EPS Conference on Controlled Fusion and Plasma Physics, Cont. Papers, vol. 19C, Part IV, Bournemouth, UK, 1995, p. 193.
[3] A.V. Anikeev, P.A. Bagryansky, P.P. Deichuli, A.A. Ivanov et al., Proc. of 24th EPS Conference on Controlled

Fusion and Plasma Physics, Berchtesgaden, Germany, 1997.
[4] E.D. Bender, G.I. Dimov, Prib. Tehn. Exper. 5 (1988) 129.
[5] E.D. Bender, Vopr. Atomn. Nauki Tehn. (Soviet VANT) Ser. Termojade. Sintez 4 (1987) 41.
[6] A.A. Ivanov et al. in: Proc. of 17th Symp. Fusion Techn. vol. 2, Rome, Italy, 1993, p. 1394.
[7] H. Kumpf et al., Annual Report 1993, Institute of Safety Research, Research Center Rossendorf, Inc., RC Rossendort: Report FZR-68 (1994) 58.
[8] K. Yatsu, Y. Nakashima et al., J. Vac. Sci. Technol. A 6 (4) (1988) 2546.
[9] Y. Nakashima, K. Yatsu, K. Tsuchiya et al., J. Nucl. Mater. 196–198 (1992) 493.
[10] D. Reiter, Randschicht-Konfigurationen von Tokamaks: Entwicklung and Anwendung stochastischer Modelle zur Beschreibung des Neutralgastransports, RC Juelich: Report Juel-1947, 1984.
[11] D. Reiter, The EIRENE Code – Users Manual, (Version: January 1992) RC Juelich: Report Juel-2599, 1992.
[12] R.K. Janev, J. Smith, Nuclear Fusion Suppl. Special Issue, 4 (1993).
[13] R.K. Janev et al., Elementary Process in Hydrogen-helium Plasmas (Springer Series on Atoms and Plasnas, vol. 4) Springer, Berlin, Heidelberg, 1987.
[14] E.W. Thomas et al., Nucl. Instr. and Meth. B 69 (1992) 427.
[15] W. Eckstein, Reflection, Nucl. Fusion Suppl. 1 (1991) 17.
[16] T. Tabata et al., Dependence of the Backscattering Coefficient of Light Ions Upon Angle of Incident, Institut of Plasma Physics, Rep. IPPJ-AM-34, Nagoya, 1984.
[17] W. Eckstein, H. Verbeek, Nuclear Fusion Suppl. Special Issue (1984) 12.
[18] D.E. Post, R. Berisch, Physics of Plasma-Wall Interaction in Controlled Fusion, NATO ASI Series B, vol. 131, New York, London, 1986.
[19] W. Eckstein, J.P. Biersack, J. Appl. Phys. A 38 (1985) 123.